Degradation of Lindane by Zero-Valent Iron Nanoparticles

Daniel W. Elliott[1]; Hsing-Lung Lien[2]; and Wei-Xian Zhang[3]

Abstract: Thus far, zero-valent iron has been studied mostly for the degradation of structurally simple one- and two-carbon halogenated organic contaminants such as chlorinated methanes, ethanes, and ethenes. In this research, laboratory synthesized particles of nanoscale iron were explored to degrade lindane, also known as γ-hexachlorocyclohexane, a formerly widely utilized pesticide and well-documented persistent organic pollutant. In general, lindane disappeared from aqueous solution within 24 h in the presence of nanoiron concentrations ranging from 0.015 to 0.39 g/L. By comparison, approximately 40% of the initial lindane dose remained in solution after 24 h in the presence of 0.53 g/L of larger microscale iron particles. However, the surface area normalized first-order rate constants were all within the same order of magnitude regardless of dose or iron type. A key reaction intermediate, γ-3,4,5,6-tetrachlorocyclohexene from dihaloelimination of lindane was identified and quantified. Trace levels of additional degradation products including benzene and biphenyl were detected but only in the high concentration experiments conducted in 50% ethanol. While up to 80% of the chlorine from the lindane molecules ended as chloride in water, only 38% of the expected chloride concentration was observed for the microscale iron experiment. This work together with previous published studies on the degradation of polychlorinated biphenyl, chlorinated benzenes, and phenols suggest that zero-valent iron nanoparticles can be effective in the treatment of more structurally complex and environmentally persistent organic pollutants such as lindane.

DOI: 10.1061/(ASCE)0733-9372(2009)135:5(317)

CE Database subject headings: Iron; Groundwater pollution; Remedial action; Pesticides; Halogen organic compounds.

Introduction

The use of nanoscale zero-valent iron (nZVI) for the remediation of groundwater impacted by a variety of contaminants including chlorinated hydrocarbons (Zhang et al. 1998; Lien and Zhang 2007, 2005, 2001, 1999; Liu et al. 2005; Lowry and Johnson 2004), nitrate (Chen et al. 2004), perchlorate (Xiong et al. 2007; Cao et al. 2005), and heavy metals (Li et al. 2008; 2007; Li and Zhang 2006; Cao and Zhang 2006; Kanel et al. 2005; Ponder et al. 2000) has received much research attention over the past decade. For the chlorinated hydrocarbons, most of this research to date has focused on relatively simple one- and two-carbon compounds including the ubiquitous solvents such as carbon tetrachloride (CCl_4), chloroform ($CHCl_3$), trichloroethene (C_2HCl_3), and tetrachloroethene (C_2Cl_4). This research has yielded numerous valuable insights regarding the mechanisms of dechlorination, kinetics, and the role of the metal surface in the degradation process. Nevertheless, much fertile research ground remains unexplored in the nZVI remediation field.

One such prospect is the amenability of nZVI to degrade and remediate persistent organic pollutants (POPs) in soil and aqueous environments. POPs, including polychlorinated biphenyls (PCBs), chlorinated benzenes, dioxins, and organochlorine pesticides such as dichlorodiphenyltrichloroethane (DDT) and lindane represent both a major public health concern and a formidable remediation challenge. By virtue of their polychlorinated structures, these contaminants tend to be only slightly soluble in water, exhibit moderate to strong sorption potentials, and are relatively recalcitrant toward biodegradation. Not surprisingly, few effective technical solutions are available to deal with this vexing problem.

The research described in this contribution focuses on the ability of iron nanoparticles to degrade lindane, a well-known organochlorine pesticide in widespread use from the 1940s until the 1990s (Walker et al. 1999; Kolpin et al. 1998). As depicted in Fig. 1, lindane has long been used in technical grade isomeric mixtures of hexachlorocyclohexanes (HCHs) or as purified γ-HCH product. Lindane and technical grade HCH were used as broad-spectrum insecticide for fruit, grain, and vegetable crops, in seed treatment, and in certain medical applications such as lice and scabies control (Walker et al. 1999). First synthesized by Michael Faraday in 1825, the HCHs apparently garnered little research or commercial attention until the early 1940s when their pesticidinal properties were discovered (Willett et al. 1998). The industrial synthesis of γ-HCH involved treating benzene with chlorine in the presence of ultraviolet light to form a mixture of isomers with a typical composition as follows: alpha (60–70%), gamma (10–12%), beta (5–12%), delta (6–10%), and epsilon (3–4%) (Willett et al. 1998; Slade 1945). The technical grade mixture could then be refined to concentrate γ-HCH, the isomer exhibiting the greatest pesticidinal activity, through a series of recrystallization steps (Slade 1945). A summary of the major physicochemical properties of lindane is provided in Table 1 (Mackay et al. 1997). For comparative purposes, data for trichloroethene and benzene are also included.

An estimated 10 million tons of technical grade HCH alone

[1]Associate, Geosyntec Consultants, 3131 Princeton Pike, Bldg. 1-B, Stee 205, Lawrenceville, NJ 08648.

[2]Associate Professor, Dept. of Civil and Environmental Engineering, National Univ. of Kaohsiung, No. 700 Kaohsiung Univ. Rd., Kaohsiung, Taiwan, ROC.

[3]Dept. of Civil and Environmental Engineering, Lehigh Univ., Bethlehem, PA, 18015 (corresponding author). E-mail: wez3@lehigh.edu

Note. Discussion open until October 1, 2009. Separate discussions must be submitted for individual papers. The manuscript for this paper was submitted for review and possible publication on October 8, 2007; approved on January 20, 2009. This paper is part of the ***Journal of Environmental Engineering***, Vol. 135, No. 5, May 1, 2009. ©ASCE, ISSN 0733-9372/2009/5-317–324/$25.00.

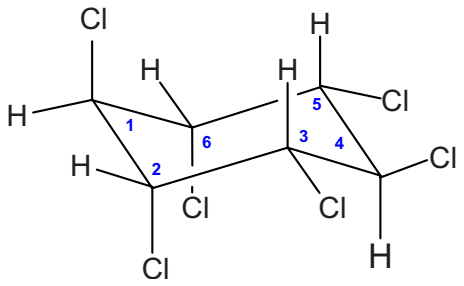

Fig. 1. Structure of γ-HCH (lindane)

has been reportedly used on a global basis between 1948 and 1997 (Walker et al. 1999). Worldwide usage of lindane over the period from 1950 to 2000 has been estimated to be 450,000 tons with approximately 63% of that total consumed in Europe, approximately 17% in Asia, and about 4.2% by the United States (Vijgen 2006). Although global usage has declined considerably since the peak levels in the 1960s and 1970s, an estimated 1.67 to 1.92 million tons of HCH residuals exist throughout the world in stockpiles, some of which are dumps or poorly constructed warehouses where the potential for soil and groundwater impact can be significant (Vijgen 2006). Moreover, the HCHs have been detected in virtually every environmental compartment around the globe, even in locales distant from their points of use (Schwarzenbach et al. 2003). Sites impacted by such contaminants tend to behave like long-term, low level sources as slow desorption from solid matrix and gradual dissolution into percolating rainfall runoff propagate continued groundwater contamination.

Despite considerable lindane-related research in the literature and the burgeoning interest in nanoscale iron, no studies involving the nZVI-mediated degradation of HCHs have, thus, far been published. The small size and large surface area translate into significantly enhanced reactivity given that these nZVI degradation reactions are surface mediated. The nZVI technology has been demonstrated to be suitable for in situ treatment of contaminant "hot-spots" given its high reactivity and flexible deployment in the field (Glazier et al. 2003; Zhang 2003; Elliott and Zhang 2001).

Herein, laboratory investigation of the dechlorination of lindane by iron nanoparticles in batch reactors is presented. Process effectiveness was assessed in terms of the identification of degradation-related intermediates and products as well as the degradation kinetics using a simplified pseudo-first order model. Valuable information on the reaction intermediates and final products has been obtained. A conceptual model of the process is proposed and the major iron-mediated degradation pathways are discussed.

Materials and Methods

Nanoparticle Synthesis

The nZVI used in this work was prepared using the well-described borohydride method in which ferrous sulfate is reduced in aqueous solution by sodium borohydride

$$2Fe^{2+}_{(aq)} + BH^{-}_{4(aq)} + 3H_2O_{(l)} \rightarrow 2Fe^{0}_{(s)} + H_2BO^{-}_{3(aq)} + 4H^{+}_{(aq)} + 2H_{2(g)} \quad (1)$$

Detailed procedures on the nZVI synthesis have been previously published (Zhang et al. 1998; Wang and Zhang 1997). The finished nanoparticles were washed with ethanol, purged with nitrogen, and refrigerated in a sealed polyethylene container under ethanol (<5%) until use. The residual water content of the nanoparticles as used typically varied between 40–50%. The nZVI used in this work was not surface modified and contained no palladium. The average particle diameter of the nanoscale iron was 60 nm, as determined by scanning electron microscopy and an acoustic/electroacoustic spectrometer.

Detailed surface characterizations of nZVI can be found in previous publications (Li and Zhang 2007; Sun et al. 2006). Specifically x-ray diffraction (XRD) analysis has confirmed the presence of both zero-valent iron and crystalline iron oxide (FeO) phases on freshly synthesized nZVI. After aging the iron for approximately 3 weeks, the x-ray absorption near edge structure (XANES) spectrum revealed the presence of 44% zero-valent iron and 56% oxidized iron (Sun et al. 2006). Thus, the surface composition of the reactive nZVI changes over time. As presented in our previous publications, the x-ray photoelectron spectroscopy (XPS) analysis indicated that other elements or impurities (borate, sodium, and carbon) were enmeshed into the iron nanoparticle matrix as a result of borohydride oxidation (Li and Zhang 2007; Sun et al. 2006).

pH/Standard Potential (E_h) Trend Experiments

The objective of these experiments was to evaluate the pH and oxidation-reduction potential (ORP) changes as a function of iron dosage, type, lindane concentration, and reaction time. In these experiments, 2,750 mL of nitrogen purged distilled water was added to a Fernbach flask fitted with a customized rubber stopper containing ports for pH and redox potential electrodes and sampling. A variable speed mixer (Heindorf) set at 600 ± 50 rpm helped to ensure well-mixed conditions. Measured dissolved oxygen levels were generally less than 0.2 mg/L after 60 min of N_2 purging. An aliquot of a lindane (97%, Aldrich) stock solution in ethanol was then spiked into the flask to yield an aqueous concentration of approximately 7.5 mg/L. Nanoscale or microscale iron was added to yield a mass concentration ranging from

Table 1. Selected Properties of Lindane, Trichloroethene, and Benzene at 25°C [Some Data from Mackay et al. (1997)]

Contaminant	Formula	Molecular weight (g/mol)	Aqueous solubility (mg/L)	Vapor pressure (Pa)	log K_{ow}	log K_{oc}
Lindane	$C_6H_6Cl_6$	290.82	6–10	0.003–0.004	2.81–3.89	1.63–4.09
Trichloroethene	C_2HCl_3	131.39	1,100	7,700–9,800	2.29	1.60–2.20
Benzene	C_6H_6	78.11	1,780	12,700	2.13	1.26–2.01

0.015 to 0.53 g/L. Prior to use, the microscale iron was mixed gently in 0.1 M HCl for approximately 30 min to remove the surface passive layer.

A combination pH electrode (Orion) was used in conjunction with a Sension1 (Hach) meter and was calibrated prior to each test. A combination Ag/AgCl reference electrode (Cole-Parmer) was used with a Model 420A pH/ORP meter (Orion) to monitor redox potential and was calibrated with fresh ZoBell solution before each test. Measured redox potential readings were converted to the standard potential E_h, the potential relative to the standard hydrogen electrode, as a function of solution temperature by adding +199 mV at 25°C (Nordstrom and Wilde 2005).

Lindane Degradation Batch Tests

In these experiments, the degradation of lindane was studied as a function of contaminant concentration, iron dosage, and iron type. The specific lindane degradation pathways were also investigated. Two experimental setups were used in this research.

The first set of experiments utilized nonbuffered distilled water containing a spike of lindane (initial concentration 7.5 mg/L) from the stock solution in ethanol; 100 mL of spiked distilled water was added to 120 mL glass amber bottles fitted with screw caps containing Teflon-lined septa. Approximately 10 mg/L of sodium azide (Fisher) was added to inhibit possible biodegradation of the contaminants. Relatively low (<1 g/L) dosages of nZVI or microscale iron powder (<10 μm, Aldrich) were then added to the reactors. The sealed reactors were placed on a rotating platform shaker at 325 rpm and 22°C and sampled at regular intervals. At each interval, 2 mL of sample was passed through a 0.20 μm syringe filter and added to 2 mL of 2,2,4-trimethylpentane in a 5 mL vial (Wheaton) fitted with an aluminum crimp cap and Teflon-lined septa. Dissolved chloride samples were also collected by adding 2 mL of syringe-filtered (0.20 μm) sample to a like volume of distilled water in a 5 mL vial.

The second set of experiments were conducted at high initial lindane concentrations (~300–600 mg/L, 1–2 mM) to identify degradation products and to elucidate potential degradation pathways. The solution consisted of 50% ethanol and 50% water to increase the solubility of lindane. The batch reactors were set up in the same manner as described previously. Much larger nZVI doses ranging from 5–25 g/L were then added to the reactors. At the desired time interval, 5 μL aliquots of sample were obtained following a brief solids settling period (<5 min) in which the reactor was placed on a circular desk magnet. Chloride samples were collected at periodic intervals as described previously. However, in this case, the matrix for the chloride samples was 50% ethanol and 50% water and the associated quantification standards used were prepared accordingly.

Analytical Procedures

A Hewlett-Packard 5890 gas chromatograph (GC) equipped with an electron capture detector and an RTX-5 (Restek) low polarity capillary column was used to quantify the aqueous concentrations of lindane and its degradation products. The column measurements were as follows: 15 m length by 0.25 mm internal diam by 0.25 μm film thickness. The carrier gas was ultrapure nitrogen flowing at 4.86 mL/min. Injection was carried out in splitless mode. The injector port and detector temperatures were 200 and 250°C, respectively. A progressive three-stage temperature ramp was used as follows: 90°C for 2 min, 90°C to 150°C at a rate of 10°C/min, 150°C to 165°C at a rate of 3°C/min, and finally 165°C to 185°C at 10°C/min. Quantification was facilitated by use of calibration curves for a series of standard solutions of known concentrations. Peak areas were measured in triplicate with relative differences less than 15%. The detection limit was below 1 μg/L.

A Shimadzu 17A GC with a Shimadzu QP-5000 mass spectrometer (MS) was used to identify and quantify the concentrations of lindane and its degradation products in ethanol. The GC was fitted with a low polarity Econocap EC-5 capillary column (Alltech). The column measurements were as follows: 30 m length by 0.25 mm internal diam by 0.25 μm film thickness. Ultrapure nitrogen flowing at 12.6 mL/min was used as the carrier gas and injections were accomplished with a split ratio of 30:1. The injector and interface temperatures were 200°C and 300°C, respectively. A two-stage temperature ramp was used as follows: 110°C for 2 min, 110°C to 200°C at a rate of 15°C/min, and 200°C to 240°C at a rate of 5°C/min. The detector sensitivity was set to 1.75 kV. Quantification was accomplished from known initial concentrations and by comparing the peak area at time t to the initial area.

Chloride samples were analyzed using a Dionex DX-120 ion chromatograph. Anion separation was accomplished by an IonPac AS-14 ion exchange column preceded by an AG-14 guard column (Dionex). The eluent consisted of a solution of 3.5 mM sodium carbonate and 1.0 mM sodium bicarbonate in deionized water. An isocratic flow rate of 1.2 mL/min was used for the chloride analyses. Quantification was facilitated by use of a calibration curve developed from a series of aqueous solutions containing 50% ethanol and known chloride concentration. Injections were generally performed in triplicate.

Brunauer-Emmett-Teller (BET) surface areas of the nanoscale iron were measured using the nitrogen adsorption method at 77 K with a Gemini 2360 surface analyzer. Prior to measurement, samples were acid washed and degassed at 250°C with a flow of N_2 (Zhang et al. 1998).

Results and Discussion

pH/E_h Trends in Aqueous Solution

Zero-valent iron Fe^0 has long been recognized as an effective electron donor regardless of its particle size. This is evidenced by the standard reduction potential (E^0) of −440 mV for the redox half-reaction between the Fe^{2+}/Fe^0 couple. In a groundwater environment, the predominant electron receptors include residual dissolved oxygen and water

$$2Fe^0_{(s)} + 4H^+_{(aq)} + O_{2(aq)} \rightarrow 2Fe^{2+}_{(aq)} + 2H_2O_{(l)} \quad (2)$$

$$Fe^0_{(s)} + 2H_2O_{(aq)} \rightarrow Fe^{2+}_{(aq)} + H_{2(g)} + 2OH^-_{(aq)} \quad (3)$$

Given its overwhelming concentration advantage as the solvent, the reduction of water at the iron surface can be expected to be the dominant redox process in groundwater. Accordingly, the iron oxidation reactions should produce a characteristic increase in solution pH and a concomitant decline in the standard potential E_h.

Table 2 summarizes observed pH and E_h changes as a function of iron dosage, type, and lindane concentration during the reaction. As shown in Table 2, the solution pH typically increased by approximately 2–3 standard units from pH ~6 to ~9. A corresponding precipitous decline in solution E_h from +400 mV to

Table 2. Comparison of pH and E_h Changes as a Function of Iron Dose, Type, and Presence of γ-HCH

Iron dose (g/L)	Iron type	[γ-HCH] (mM)	$pH_{initial}/pH_{final}$	ΔpH	$E_{h,initial}/E_{h,final}$ (mV)	ΔE_h (mV)
0.11	Nano	0	5.20/8.66	3.46	+372.0/−438.1	−810.1
0.10	Nano	0.026	5.07/7.97	2.90	+398.6/−417.7	−816.3
0.39	Nano	0	6.21/8.71	2.50	+391.4/−489.7	−881.1
0.39	Nano	0.023	6.31/9.07	2.76	+427.2/−430.4	−857.6
0.53	Micro	0.024	6.50/8.52	2.02	+407.0/−316.1	−723.1

approximately −490 mV was also observed. In addition, the magnitude of the pH increase for the microscale iron was fully 0.5 to 1.5 units less than that achieved with nZVI. Similarly, the magnitude of the E_h decline was approximately 100 to 150 mV less for the microscale iron dosage as compared to those with nZVI.

Over a reasonable range of ferrous iron [Fe(II)] concentrations from 0.5 to 10 mg/L, the equilibrium E_h of the system should be on the order of −550 mV to −520 mV as indicated in the E_h/pH diagram depicted in Fig. 2. These equilibrium values do not differ appreciably from the observed E_h range of −415 to −490 mV observed after an elapsed time of approximately 115 min. The circular markers in Fig. 2 represent the observed E_h and pH data at elapsed times of 0, 1, 5, 10, 20, 30, and 100 min for a representative dosage (0.21 g/L) of nZVI in distilled water. They lead into the equilibrium E_h/pH stability zone, which is remarkably small given the range of nZVI dosages (e.g., from 0.015 to 0.39 g/L) it encompasses. Interestingly, this area was sufficiently reducing as to be near the lower stability limit of water (E_h= −532 mV at pH∼9) and favorable for the generation of hydrogen gas. In this context, the addition of iron nanoparticles can stimulate both chemically and biologically induced dechlorination.

With respect to Fig. 2, a strong thermodynamic driving force exists for the reduction of lindane in the iron-water system. Since the estimated standard reduction potentials vary from +500 to +1,500 mV for various one-carbon alkyl halides at pH 7, the reduced forms of these species should be expected under equilibrium conditions (Stumm and Morgan 1996; Gillham and O'Hannesin 1994; Vogel et al. 1987). Thus, at equilibrium, polyhalogenated species such as lindane would be expected to undergo rapid facile reduction in the nZVI-water system.

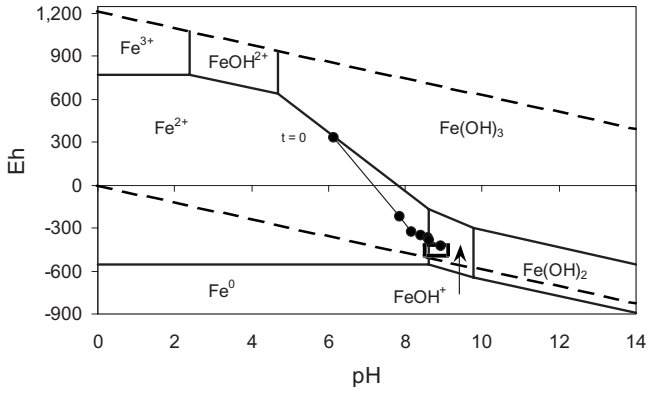

Fig. 2. Equilibrium E_h/pH diagram for the aqueous nanoiron system at 25°C. The total dissolved iron concentration is 0.5 mg/L. The circular markers signify the pH/E_h profile at elapsed time of 0, 1, 5, 10, 20, 30, and 100 min after addition of 0.21 g/L nFe. The rectangular region containing the t=100 min marker represents the observed equilibrium stability zone for the 0.015–0.39 g/L additions of nFe.

Degradation of Lindane

As depicted in Fig. 3, greater than 95% of the lindane (initial concentration 7.5 mg/L) was removed from aqueous solution within 24 h at relatively low nZVI loadings of 0.10 to 0.39 g/L while 60% was removed at 0.015 g/L. The control reactor containing no nZVI (pH=6.91) exhibited an apparent early loss of lindane possibly due to sorption to the glass surface. However, normalized concentrations (C/C_0) generally exceeded 0.80–0.85 indicating that abiotic and biotic losses were not significant during the course of the experiments. Although the extent of lindane removal depended on the iron loading over the initial 10 h of the experiment, the 0.10 and 0.39 g/L doses yielded similar results by its conclusion (∼24 h). This suggests that the extent of contaminant transformation is largely independent of nZVI dose except at relatively short (<24 h) contact times. The nanoscale iron particles proved to be quite effective in degrading lindane. On the other hand, the particle size of the iron strongly influenced the observed extent of lindane degradation as all of the nZVI doses performed significantly better than the 0.53 g/L microscale iron dose. After 24 h, fully 43% of lindane still remained in the aqueous solution.

Obviously, the loss of lindane from aqueous solution does not necessarily mean that it has been transformed. As demonstrated in Fig. 4, the disappearance of lindane was accompanied by the observation of one major degradation product identified as γ-3,4,5,6-tetrachlorocyclohexene (TeCCH) using the NIST62 pesticides library. TeCCH has also been reported as the

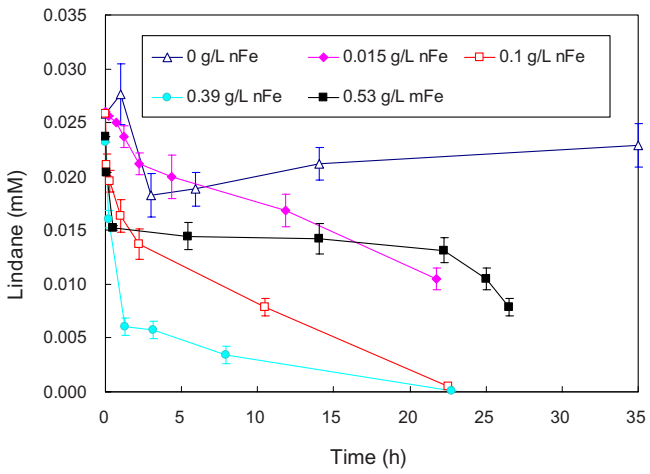

Fig. 3. γ-HCH removal from aqueous solution as a function of iron dose and type

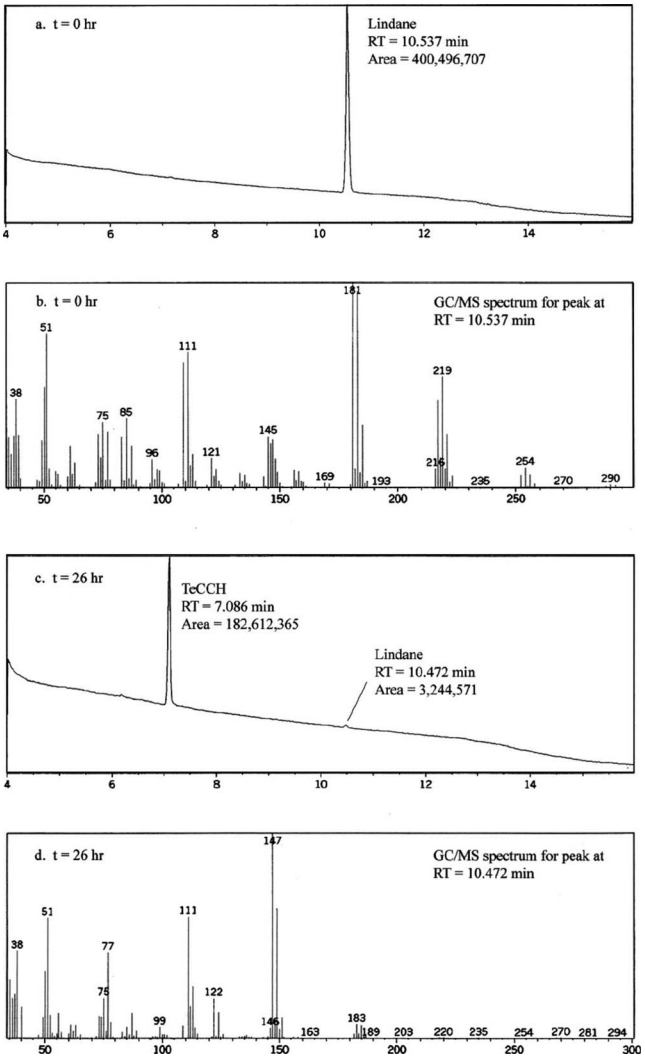

Fig. 4. Representative GC and GC/MS chromatograms from the nanoiron mediated degradation of lindane in ethanol at various reaction times. The major intermediate identified was confirmed to be 3,4,5,6-tetrachlorocyclohexene (TeCCH)

major intermediate in the anaerobic biodegradation of lindane (Middeldorp et al. 1996; Buser and Muller 1995; Ohisa et al. 1980; Jagnow et al. 1977; Beland et al. 1976) and in the electrochemical reduction of lindane (Beland et al. 1976). In our experiments, the presence of sodium azide in the batch reactors should have inhibited microbial activity such that the reductions observed were mediated by the iron surface. TeCCH was also detected in a recent study in which the abiotic transformation of lindane by FeS was investigated (Liu et al. 2003). Curves depicting the observed TeCCH concentration as a function of iron dose and type are presented in Fig. 5. Because TeCCH did not accumulate over the course of the experiments, it is likely that it is further degraded. Maximum TeCCH concentrations were observed within the initial 5 h of the experiments and were typically on the order of 15% or less of the stoichiometric equivalent of lindane. Beland et al. (1976) observed a very similar TeCCH concentration trend in the electrochemical reduction of lindane in dimethyl sulfoxide under an applied voltage of −1.520 V (versus the standard calomel electrode).

Relatively few organic degradation products were observed in the batch reactors. Low levels of benzene and biphenyl were

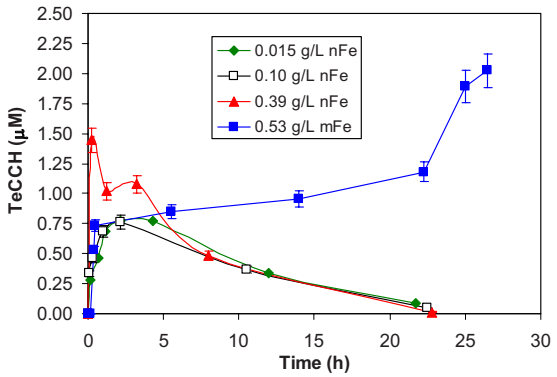

Fig. 5. Concentration profiles of TCCH as a function of iron dose and type

detected in the high concentration degradation tests conducted in ethanol. Interestingly, benzene was detected as a stable end product in the anaerobic biodegradation of lindane (Middeldorp et al. 1996; Beland et al. 1976); γ-pentachlorocyclohexene (PCCH) was also identified at trace levels. Several investigators have reported observing PCCH during the base-catalyzed dehydrohalogenation of lindane to a mixture of base-stable trichlorobenzenes, particularly the 1,2,4-isomer (Ngabe et al. 1993; Cristol et al. 1951). Secondary alkyl halides such as lindane undergo relatively facile nonreductive E_2 elimination by hydroxide (Hughes and Ingold 1941). Ngabe et al. (1993) reported a half-life for lindane of 6.3 days in a buffered aqueous solution of pH 9.01 and 30°C. The lack of dehydrohalogenation intermediates and end products observed during our experiments suggests that base-catalyzed elimination was not an important transformation mechanism under the conditions studied. Finally, trace levels of a transient cyclohexadiene derivative were periodically observed in the ethanol reactors. While this potential intermediate could not be conclusively identified, its observed GC/MS spectrum showed a major peak at an m/e ratio of 79 and minor peaks at m/e 114 and 149 consistent with a dichlorocyclohexadiene (DCCHD).

The major inorganic end products of the nZVI-mediated degradation of lindane included ferrous iron and chloride. The chloride data are shown in Fig. 6. For the nZVI experiments, the observed chloride concentrations accounted for approximately 80% of the chloride expected from the complete degradation of lindane, assuming 6 moles of chloride evolved per mole of lindane. However, less than 38% of the expected chloride concentration was observed for the microscale iron experiment. The generation of aqueous chloride provides ultimate evidence of dechlorination. Not surprisingly, the iron nanoparticles produced a higher degree of dechlorination than did the microscale iron.

Reaction Kinetics

In previous literature, the pseudo-first-order kinetics model has been most frequently used to characterize the iron-mediated degradation of redox-amenable contaminants (Johnson et al. 1996). This approach has been used with some success for simple 1- and 2-carbon chlorinated hydrocarbons, particularly in terms of the surface area normalized pseudo-first-order rate constant, k_{SA}. As applied to lindane, the pseudo-first-order kinetics equation is as follows:

$$\frac{d[\gamma - \mathrm{HCH}]}{dt} = -k_{\mathrm{obs}}[\gamma - \mathrm{HCH}] \quad (4)$$

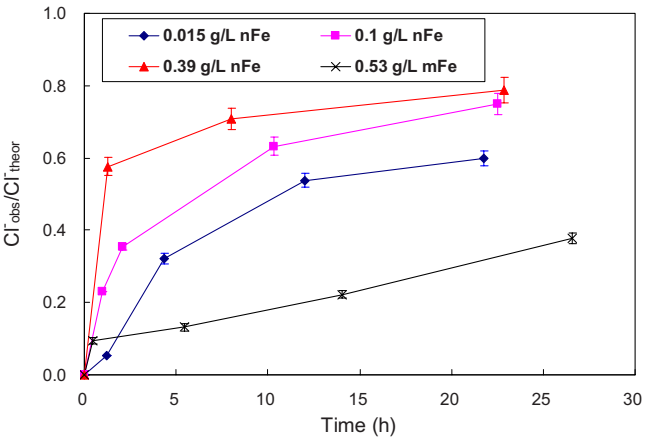

Fig. 6. Concentration profiles of observed chloride as a function of iron dose and type. The observed chloride data are normalized to the stoichiometric equivalent of chloride produced assuming complete conversion from γ-HCH.

$$\frac{d[\gamma - \mathrm{HCH}]}{dt} = -k_{SA} a_s \rho_{Fe} [\gamma - \mathrm{HCH}] \tag{5}$$

where k_{obs}=observed pseudo-first-order rate constant (1/h); k_{SA} =surface area-normalized reaction rate coefficient ($L/h/m^2$); a_s=specific surface area of nZVI (m^2/g), and ρ_{Fe}=nZVI concentration (g/L). A specific surface area of 33.5 m^2/g determined by the BET method for dry iron nanoparticles was used in our calculations (Zhang et al. 1998; Sun et al. 2006).

As expected, the first-order rate constants for the nZVI doses were considerably larger than that for the microscale iron dose. As summarized in Table 3, the two larger nZVI doses, 0.10 and 0.39 g/L, exhibited k_{obs} values of 0.149 and 0.138 1/h, respectively. The k_{obs} value for the lowest nZVI dose, 0.015 g/L was lower by a factor of approximately 4, suggesting a rough dependence of reaction rate on iron dose. Interestingly, the surface area normalized first-order rate constants, k_{SA}, are somewhat all within the same order of magnitude regardless of dose or iron type. The observed k_{SA} data ranged from 1.13×10^{-2} $L/h/m^2$ for the 0.53 g/L does of microscale iron to 7.20×10^{-2} $L/h/m^2$ for the 0.015 g/L nZVI dose. Obviously, the data set is not sufficiently large to warrant a detailed investigation of this possible trend.

However, it has been reported that nZVI may not be more reactive than mZVI on a surface area normalized basis for carbon tetrachloride reduction (Nurmi et al. 2005). Another compounding factor is the strong tendency of nZVI to aggregate, which can result in a varying and potentially lessening of a_S over time, which can further affect calculations of k_{SA}. Lowry et al. (2007) recently investigated the effects of aggregation on nZVI sedimentation. This issue is of profound importance to nZVI manufacturing, deployment in the field, reactivity, and fate and transport within the subsurface.

Table 3. Summary of Batch Data from the First-Order Kinetics Model

Iron type	Iron dose (g/L)	k_{obs} (1/h)	k_{SA} ($L/h/m^2$)
Nano	0.015	3.62×10^{-2}	7.20×10^{-2}
Nano	0.10	1.49×10^{-1}	4.46×10^{-2}
Nano	0.39	1.38×10^{-1}	1.05×10^{-2}
Micro	0.53	6.00×10^{-3}	1.13×10^{-2}

The first-order model did not adequately describe the degradation of lindane by iron nanoparticles in our batch reactors. The pseudo-first-order model fit was not too far off for the lowest dosage of nZVI (0.015 g/L) but the fit grew progressively worse with increasing iron dose and was particularly inadequate for the microscale iron dose. The fits for all iron doses exhibited considerable deviation from first-order behavior during the initial several hours of the reactions when the aqueous lindane concentrations were the highest.

This deviation can be partially explained in terms of the dual removal processes, sorption to the nZVI, and reduction at the surface. Since the concentration of lindane and TeCCH was not evaluated on the surface of iron, the k_{SA} data can be thought of in terms of a "lumped" parameter but sorption was generally only a factor during the initial stages of the experiment. This suggests that the sorption of lindane at the iron surface may account for a noticeable potion for the disappearance of lindane in the aqueous solution. It has been reported that the sorption process affects the kinetic analysis for the dechlorination of halogenated ethenes with ZVI (Burris et al. 1995).

Proposed Degradation Pathway and Conceptual Model

As observed in this study, TeCCH is the principal degradation intermediate produced by the iron-mediated degradation of lindane. TeCCH is generated by the dihaloelimination of vicinal chlorides from carbons 1 and 2 of lindane as follows:

$$C_6H_6Cl_6 + Fe^0 \rightarrow C_6H_6Cl_4 + Fe^{2+} + 2Cl^- \tag{6}$$

Both chlorine atoms occupy axial positions on their respective carbon centers and are oriented antiperiplanar (dihedral angle of 180°), which maximizes their propensity toward reduction (Smith and March 2001). Based upon the prolonged observance of TeCCH and the only transient appearance of subsequent potential intermediates, it appears that this initial reduction step is rate controlling. The two subsequent dihaloelimination steps are believed to occur more rapidly ultimately yielding benzene, ferrous iron, and chloride as major end products. The overall pathway for the iron-mediated reduction of lindane to benzene is depicted in Fig. 7.

The reduction sequence is depicted in Fig. 8. Aqueous (or from ethanol-water solution) lindane must first sorb onto the iron surface before any reaction can occur. Once sorbed, the highly electronegative chlorine substituents act as the electron acceptors while Fe^0 serves as the electron donor. The reduction product, TeCCH can then undergo further sequential reductions ultimately yielding benzene, or it can desorb into bulk aqueous solution. However, as has been mentioned previously, besides γ-TeCCH, no further degradation-related intermediates or products (e.g., benzene) were observed in the aqueous experiments. The reduction of alkyl halides such as lindane typically proceeds via a series of two discrete single electron transfers (Roberts et al. 1996; Vogel et al. 1987). In the first step, an electron from Fe^0 is donated to the surface-associated lindane forming a neutral radical as one chloride ion is simultaneously ejected. Another electron is then lost from the transient Fe^+ species to the reacting carbon center of the radical, which then undergoes double bond formation and simultaneous loss of chloride from the beta carbon. In this manner, Fe^{2+} and TeCCH are produced along with the evolution of two Cl^- ions. A similar sequence of single electron transfers is expected to occur during the generation of the subsequent degradation products. To some degree, the mechanisms il-

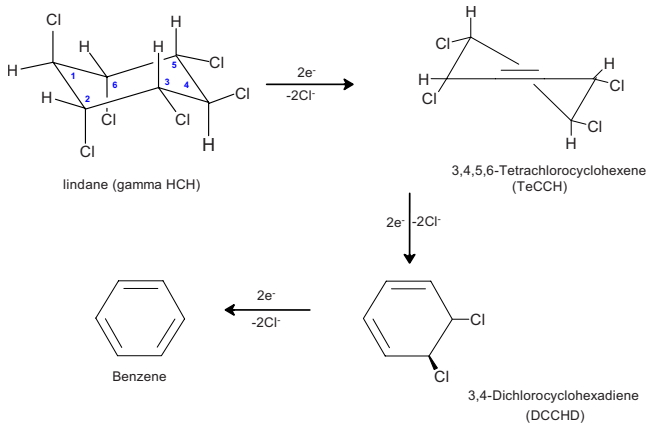

Fig. 7. Dihaloelimination degradation pathway from lindane to benzene; implicit vinyl and aromatic hydrogen atoms are not shown. The structure of TeCCH (a six-carbon "twisted boat") features two implicit carbon atoms on either side of the double bond; implicit aliphatic hydrogen atoms on DCCHD are not shown to improve clarity.

lustrated in Fig. 8 are similar to those proposed by Liu et al. for the FeS-mediated reduction of lindane although the observed degradation products differ (Liu et al. 2003).

Cost Analysis for Zero-Valent Iron Nanoparticles

Prior to 2000, there were no commercial suppliers of iron nanoparticles in the United States or elsewhere around the world. Small quantities (e.g., <10 kg) were synthesized in the laboratory, usually using the now well-described borohydride reduction process for both bench-scale and pilot-scale tests. Given the lack of any economies of scale, the fact that the synthesis was performed in a laboratory setting, and the labor-intensive nature of the process, the costs to produce the nZVI was significant (e.g., $>\$250$/kg). Since that time, several vendors have started limited production of iron nanoparticles. As a consequence, the price is decreasing markedly. Data obtained from one nZVI manufacturer indicated that nZVI costs were on the order of $\$50$/kg as of mid-2004. However, even with an increased supply of nZVI

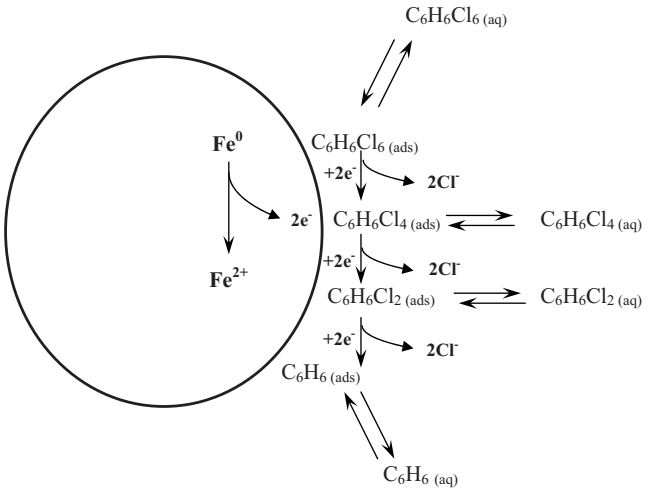

Fig. 8. Conceptual model of the degradation of lindane by nanoscale iron

available and a lower price point, the general perception is that the nanoparticle technology is still too expensive for widespread utilization by environmental remediation practitioners. While an analysis of surface area per unit cost could result in a more favorable analysis for nZVI, the fact that particle aggregation can cause the specific surface area to vary, limits the effectiveness of the approach. As surface-modified nZVI products are developed and field evaluated, this alternative costing approach should be revisited.

Conclusions

This work demonstrates that lindane can be effectively degraded with zero valent iron nanoparticles in both aqueous solution and in ethanol-water systems. The extent of lindane transformation was appreciably greater for the nZVI doses as compared with commercially available microscale iron powders (~ 10 μm) at similar iron dosages. However, the surface area normalized first order rate constants are somewhat all within the same order of magnitude regardless of dose or iron type. The degradation of lindane proceeded through γ-3,4,5,6-tetrachlorocyclohexene, a dihaloelimination product in both the aqueous experiments and the "high concentration" studies conducted in ethanol water. No nonhalogenated organic end products were detected in the aqueous experiments, but trace concentrations of benzene were detected in the ethanol-water system. Chloride was detected as a stable end product in both systems, demonstrating the reductive degradation of lindane.

Despite these promising results, additional studies are warranted to better characterize the kinetics of the degradation process, more rigorously investigate and characterize the degradation pathways and intermediates, and evaluate the efficacy of the nZVI technology on sorbed or surface-associated lindane under field conditions.

Acknowledgments

Research described in this work has been supported by the Pennsylvania Infrastructure Technology Alliance (PITA) and by the U.S. Environmental Protection Agency (EPA STAR Grant Nos. R829625 and GR832225).

References

Beland, F. A., Farwell, S. O., Robocker, A. E., and Geer, R. A. (1976). "Electrochemical reduction and anaerobic degradation of lindane." *J. Agric. Food Chem.*, 24(4), 753–756.

Burris, D. R., Campbell, T. J., and Manoranjan, V. S. (1995). "Sorption of trichloroethylene and tetrachloroethylene in a batch reactive metallic iron-water system." *Environ. Sci. Technol.*, 29(11), 2850–2855.

Buser, H. R., and Muller, M. D. (1995). "Isomer and enantioselective degradation of hexachlorocyclohexane isomers in sewage sludge under anaerobic conditions." *Environ. Sci. Technol.*, 29(3), 664–672.

Cao, J., Elliott, D., and Zhang, W. (2005). "Perchlorate reduction by nanoscale iron particles." *J. Nanopart. Res.*, 7(4–5), 499–506.

Cao, J., and Zhang, W. X. (2006). "Stabilization of chromium ore processing residue (COPR) with nanoscale iron particles." *J. Hazard. Mater.*, 132(2–3), 213–219.

Chen, S.-S., Hsu, H.-D., and Li, C.-W. (2004). "A new method to produce nanoscale iron for nitrate removal." *J. Nanopart. Res.*, 6(6), 639–647.

Cristol, S. J., Hause, N. L., and Meek, J. S. (1951). "Mechanisms of

elimination reactions. The kinetics of the alkaline dehydrochlorination of the benzene hexachloride isomers." *J. Am. Chem. Soc.*, 73(2), 674–679.
Elliott, D. W., and Zhang, W. X. (2001). "Field assessment of nanoscale biometallic particles for groundwater treatment." *Environ. Sci. Technol.*, 35(24), 4922–4926.
Gillham, R. W., and O'Hannesin, S. F. (1994). "Enhanced degradation of halogenated aliphtics by zero-valent iron." *Ground Water*, 32(6), 958–967.
Glazier, R., Venkatakrishnan, R., Gheorghiu, F., Walata, L., Nash, R., and Zhang, W. X. (2003). "Nanotechnology takes root." *Civ. Eng. (N.Y.)*, 73(5), 64–69.
Hughes, E. D., and Ingold, C. K. (1941). "The mechanism and kinetics of elimination reactions." *Trans. Faraday Soc.*, 37, 657–685.
Jagnow, G., Haider, K., and Ellwardt, P. (1977). "Anaerobic dechlorination and degradation of hexachlorocyclohexane isomers by anaerobic and facultative anaerobic bacteria." *Arch. Microbiol.*, 115(3), 285–292.
Johnson, T. L., Scherer, M. M., and Tratnyek, P. G. (1996). "Kinetics of halogenated organic compound degradation by iron metal." *Environ. Sci. Technol.*, 30(8), 2634–2640.
Kanel, S. R., Manning, B., Charlet, L., and Choi, H. (2005). "Removal of arsenic(III) from groundwater by nanoscale zero-valent iron." *Environ. Sci. Technol.*, 39(5), 1290–1298.
Kolpin, D. W., Barbash, J. E., and Gilliom, R. J. (1998). "Occurrence of pesticides in shallow groundwater of the United States: Initial results from the national water-quality assessment program." *Environ. Sci. Technol.*, 32(5), 558–566.
Li, X. Q., Cao, J. S., and Zhang, W. X. (2008). "Immobilization of hexavalent chromium with iron nanoparticles: Characterizations with high resolution x-ray photoelectron spectroscopy (HR-XPS)." *Ind. Eng. Chem. Res.*, 47(7), 2131–2139.
Li, X. Q., and Zhang, W. X. (2006). "Iron nanoparticles: The core-shell structure and unique properties for Ni(II) sequestration." *Langmuir*, 22(11), 4638–4642.
Li, X. Q., and Zhang, W. X. (2007). "Sequestration of metal cations with zerovalent iron nanoparticles—A study with high resolution x-ray photoelectron spectroscopy (HR-XPS)." *J. Phys. Chem. C*, 111(19), 6939–6946.
Lien, H. L., and Zhang, W. X. (1999). "Transformation of chlorinated methanes by nanoscale iron particles." *J. Environ. Eng.*, 125(11), 1042–1047.
Lien, H. L., and Zhang, W. X. (2001). "Nanoscale iron particles for complete reduction of chlorinated ethenes." *Colloids Surf., A*, 191(1–2), 97–105.
Lien, H. L., and Zhang, W. X. (2005). "Hydrodechlorination of chlorinated ethanes by nanoscale Pd/Fe bimetallic particles." *J. Environ. Eng.*, 131(1), 4–10.
Lien, H. L., and Zhang, W. X. (2007). "Nanoscale Pd/Fe bimetallic particles: Catalytic effects of palladium on hydrodechlorination." *Appl. Catal., B*, 77(1–2), 110–116.
Liu, X., Peng, P. A., Fu, J., and Huang, W. (2003). "Effects of FeS on the transformation kinetics of γ-hexachlorocyclohexane." *Environ. Sci. Technol.*, 37(7), 1822–1828.
Liu, Y., Majetich, S. A., Tilton, R. D., Sholl, D. S., and Lowry, G. V. (2005). "TCE dechlorination rates, pathways, and efficiency of nanoscale iron particles with different properties." *Environ. Sci. Technol.*, 39(5), 1338–1345.
Lowry, G. V., and Johnson, K. M. (2004). "Congener-specific dechlorination of dissolved PCBs by microscale and nanoscale zerovalent iron in a water/methanol solution." *Environ. Sci. Technol.*, 38(19), 5208–5216.
Lowry, G. V., Phenrat, T., Saleh, N., Sirk, K., and Tilton, R. (2007). "Aggregation and sedimentation of aqueous nanoscale zerovalent iron dispersions." *Environ. Sci. Technol.*, 41(1), 284–290.
Mackay, D., Shiu, W.-X., and Ma, K.-C. (1997). "Insecticides." *Illustrated handbook of physical-chemical properties and environmental fate for organic chemicals*, Vol. V, Lewis Publishers, New York, 3898–3915.
Middeldorp, J. M., Jaspers, M., Zehnder, J. B., and Schraa, G. (1996). "Biotransformation of α-, β-, γ-, and δ-hexachlorocyclohexane under methanogenic conditions." *Environ. Sci. Technol.*, 30(7), 2345–2349.
Ngabe, B., Bidleman, T. F., and Falconer, R. (1993). "Base hydrolysis of alpha- and gamma-hexachlorocyclohexanes." *Environ. Sci. Technol.*, 27(9), 1930–1933.
Nordstrom, D. K., and Wilde, F. D. (2005). "Reduction-oxidation potential (electrode method)." *National field manual for the collection of water-quality data*, U.S. Geological Survey.
Nurmi, J. T., et al. (2005). "Characterization and properties of metallic iron nanoparticles: Spectroscopy, electrochemistry, and kinetics." *Environ. Sci. Technol.*, 39(5), 1221–1230.
Ohisa, N., Yamaguchi, M., and Kurihara, N. (1980). "Lindane degradation by cell-free extracts of clostridium rectum." *Arch. Microbiol.*, 125(3), 221–225.
Ponder, S. M., Darab, J. G., and Mallouk, T. E. (2000). "Remediation of Cr(VI) and Pb(II) aqueous solution using supported nanoscale zero-valent iron." *Environ. Sci. Technol.*, 34(12), 2564–2569.
Roberts, A. L., Totten, L. A., Arnold, W. A., Burris, D. R., and Campbell, T. J. (1996). "Reductive elimination of chlorinated ethylenes by zero valent metals." *Environ. Sci. Technol.*, 30(8), 2654–2659.
Schwarzenbach, R. P., Gschwend, P. M., and Imboden, D. M. (2003). "An introduction to environmental organic chemicals." *Environmental organic chemistry*, 2nd Ed., Wiley, New York, 36–37.
Slade, R. E. (1945). "The γ-isomer of hexachlorocyclohexane (gammexane): An insecticide with outstanding properties." *Chem. Ind.*, 40, 314–319.
Smith, M. B., and March, J. (2001). "Eliminations." *March's advanced organic chemistry*, 5th Ed., Wiley, New York, 1299–1376.
Stumm, W., and Morgan, J. J. (1996). "Oxidation and reduction: Equilibria and microbial mediation." *Aquatic chemistry*, 3rd Ed., Wiley, New York, 425–507.
Sun, Y. P., Li, X. Q., Cao, J., Zhang, W. X., and Wang, H. P. (2006). "Characterization of zero-valent iron nanoparticles." *Adv. Colloid Interface Sci.*, 120(1–3), 47–56.
Vijgen, J. (2006). "Overview historical HCH/Lindane production and occurring HCH-residuals." *The legacy of lindane HCH isomer production, Main Rep.*, Int. HCH and Pesticides Association (IHPA), 18–19.
Vogel, T. M., Criddle, C. S., and McCarty, P. L. (1987). "Transformations of halogenated aliphatic compounds." *Environ. Sci. Technol.*, 21(8), 722–736.
Walker, K., Vallero, D. A., and Lewis, R. G. (1999). "Factors influencing the distribution of lindane and other hexachlorocyclohexanes in the environment." *Environ. Sci. Technol.*, 33(24), 4373–4378.
Wang, C. B., and Zhang, W. X. (1997). "Synthesizing nanoscale iron particles for rapid and complete dechlorination of TCE and PCBs." *Environ. Sci. Technol.*, 31(7), 2154–2156.
Willett, K. L., Ulrich, E. M., and Hites, R. A. (1998). "Differential toxicity and environmental fates of hexachlorocyclohexane isomers." *Environ. Sci. Technol.*, 32(15), 2197–2207.
Xiong, Z., Zhao, D., and Pan, G. (2007). "Rapid and complete destruction of perchlorate in water and ion-exchange brine using stabilized zero-valent iron nanoparticles." *Water Res.*, 41(15), 3497–3505.
Zhang, W. X. (2003). "Nanoscale iron particles for environmental remediation: An overview." *J. Nanopart. Res.*, 5(3–4), 323–332.
Zhang, W. X., Wang, C. B., and Lien, H. L. (1998). "Treatment of chlorinated organic contaminants with nanoscale bimetallic particles." *Catal. Today*, 40(4), 387–395.